

## Multiple Exciton Generation by a Single Photon in Single-Walled Carbon Nanotubes

Satoru Konabe and Susumu Okada

*Graduate School of Pure and Applied Sciences, University of Tsukuba, Tsukuba, Ibaraki 305-8571, Japan  
and CREST, Japan Science and Technology Agency, 7 Gobancho, Chiyoda, Tokyo 102-0076, Japan*

(Received 21 July 2011; published 29 May 2012)

Multiple-exciton generation in single-walled carbon nanotubes is investigated theoretically. We show that multiple excitons can be directly generated by a single photon through resonant coupling with multiexciton states. Further, the theoretically predicted threshold energy for this process is consistent with recent experimental results. Our calculations clarify the elementary processes of multiple-exciton generation in single-walled carbon nanotubes.

DOI: [10.1103/PhysRevLett.108.227401](https://doi.org/10.1103/PhysRevLett.108.227401)

PACS numbers: 78.67.Ch, 71.35.Cc

To realize an environmentally sustainable society, it is important to develop novel devices that have low energy consumptions to reduce the depletion of natural energy sources. It is also important to investigate and develop clean, renewable natural energy sources. Solar power is one of the most promising inexhaustible natural energy sources. In recent decades, much effort has been devoted to developing solar cells and to increasing their energy conversion efficiencies. Although recent technical progress has made it possible to utilize solar cells to power industrial applications, Shockley and Queisser [1] revealed that there is a fundamental limit on the energy conversion efficiency, which is determined by the detailed balance of various processes.

Of the various processes that contribute to energy dissipation, photoelectric conversion mainly determines the energy conversion efficiency of cells. In conventional bulk semiconductors, a single electron-hole pair or an exciton is generated on the absorption of a single photon whose energy exceeds that of the energy gap between the conduction and valence bands. In this process, the surplus photon energy is dissipated through phonon emission as heat. However, two or more electron-hole pairs or excitons can be generated through energy transfer mediated by the Coulomb interaction if such a process can be much more efficient than the dissipative process associated with phonons. It is known as multiple-exciton generation (MEG). Since it generates two or more electron-hole pairs, MEG may substantially enhance the energy conversion efficiency. It is thus important to clarify the underlying process of MEG, not only to develop next-generation photovoltaic devices that exceed the Shockley-Queisser limit, but also to understand the fundamental physics of strongly interacting many-body excited states.

It was predicted that MEG is efficient in semiconducting nanocrystals due to inefficient phonon emission, known as the phonon bottleneck [2]. The discretized energy levels of semiconducting nanocrystals hinder resonance with the phonon energy due to the energy differences that exist between these levels. Furthermore, while energy is

conserved, momentum is not necessarily conserved due to the absence of translational symmetry in the nanocrystals. Therefore, in semiconducting nanocrystals, MEG overcomes the relaxation of photoexcited states caused by phonon emission. Indeed, MEG has been experimentally observed in several semiconductor nanocrystals [3–6]. However, contrary to the above reports, recent experiments indicate that MEG in confined materials does not exceed the efficiency in the corresponding bulk systems [7–12]. While various theories have been proposed regarding the efficiency and the threshold energy, the mechanism of MEG in semiconducting nanocrystals is still controversial [13–20].

In addition to semiconducting nanocrystals, single-walled carbon nanotubes (SWNTs) are another possible system for investigating MEG since their quasi-one-dimensional structure gives rise to a substantial Coulomb interaction [21–23]. SWNTs can be used to systematically analyze the fundamental mechanism of MEG since their sizes and structures have been well characterized. One of the most important difference between nanocrystals and SWNTs is the conservation restriction applying for the MEG process. The MEG of nanocrystals obeys only energy conservation, while the MEG of SWNTs obeys the energy conservation, momentum conservation, and the angular momentum conservation. The difference of dimensionality, accordingly, can allow us to determine the microscopic processes of MEG in SWNTs. MEG has recently been observed in SWNTs by transient absorption spectroscopy [24,25] and photocurrent spectroscopy [26]. However, as is the case with semiconductor nanocrystals, the underlying physics of MEG in SWNTs has not yet been determined.

In this study, we, thus, theoretically determine the fundamental process of MEG in SWNTs. We show that MEG occurs in SWNTs by the direct photogeneration of multiple excitons. In addition, we also demonstrate that the high efficiency of MEG is due to the strong Coulomb interaction between excitons and to a singularity in the density of states of multiple-exciton states. This study provides a

specific criterion for distinguishing the microscopic mechanisms of MEG in SWNTs.

We consider direct photo-induced generation of multiple excitons. Of the various possible multiple-exciton states, we consider only two-exciton final states. A single photon can generate two excitons due to resonant coupling between the single-exciton state and the multiple-exciton state induced by the Coulomb interaction. The perturbation theory has successfully explained, for instance, the Auger recombination rate of excitons in SWNTs [27], which justified the perturbation treatment of the Coulomb interaction between interacting excitons. After utilizing the first order perturbation regarding the Coulomb interaction  $V$ , the ground state  $|g\rangle$  becomes

$$|\tilde{g}\rangle = |g\rangle + \sum_{\mu} |\mu\rangle \frac{\langle \mu | V | g \rangle}{E_0 - E_{\mu}} + \sum_{\mu, \nu} |\mu; \nu\rangle \frac{\langle \mu; \nu | V | g \rangle}{E_0 - E_{\mu, \nu}}, \quad (1)$$

and the two-exciton state,  $|\mu; \nu\rangle$ , becomes

$$|\widetilde{\mu; \nu}\rangle = |\mu; \nu\rangle + \sum_{\mu'} |\mu'\rangle \frac{\langle \mu' | V | \mu; \nu \rangle}{E_{\mu, \nu} - E_{\mu'}} \times \sum_{\mu', \nu' \neq \mu, \nu} |\mu'; \nu'\rangle \frac{\langle \mu'; \nu' | V | \mu; \nu \rangle}{E_{\mu, \nu} - E_{\mu', \nu'}}. \quad (2)$$

In the above equations,  $|\mu\rangle \equiv |n, q\rangle$  and  $|\mu; \nu\rangle \equiv |n, q; n', q'\rangle = |n, q\rangle \otimes |n', q'\rangle$ , where  $|n, q\rangle = \sum_k Z_{k,q}^n c_{c,k}^{\dagger} c_{v,(k-q)} |g\rangle$  ( $n = 1, 2, \dots$ ) is the  $n$ th exciton state with momentum  $q$  whose energy is denoted by  $E_{\mu} \equiv E_q^n$ . The energy of two-exciton state is defined by  $E_{\mu, \nu} \equiv E_q^n + E_{q'}^{n'}$ . Here,  $c_{c(v)}$  is the annihilation operators for an electron in the conduction (valence) band. The amplitude of excitons,  $Z_{k,q}^n$ , and its energy  $E_q^n$  are determined below by solving the Bethe-Salpeter equation.

As a result of the Coulomb interaction, the multiple-exciton state can directly couple to the ground state by absorbing a single photon, i.e.,  $\langle g | \mathcal{H}_{\text{op}} | \mu; \nu \rangle \neq 0$ . The direct generation of two excitons by a single photon is forbidden by the selection rule, as shown in Fig. 1. Using the perturbed states (1) and (2), the MEG rates are calculated by the following expression of the Fermi golden rule [13]:

$$\Gamma_{\text{MEG}}(\omega) = \frac{2\pi}{\hbar} \sum_q \left| \sum_n \frac{\langle g | \mathcal{H}_{\text{op}} | n, 0 \rangle \langle n, 0 | V | 1, q; 1, -q \rangle}{E_q^1 + E_{-q}^1 - E_0^n + i\gamma} \right|^2 \times \delta(\hbar\omega - E_q^1 - E_{-q}^1). \quad (3)$$

We assume that the two excitons in the final state do not interact with each other. Resonant coupling between the excited states of the single-exciton and the multiexciton state is characterized by the following perturbation process (see Fig. 1). First, the excited states of a single exciton with zero momentum  $|n, 0\rangle$  are generated by the exciton-photon interaction, which is denoted by  $\mathcal{H}_{\text{op}}$ . These excited states

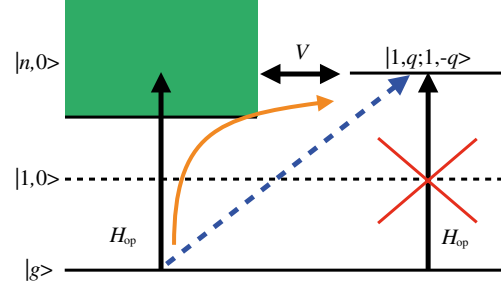


FIG. 1 (color online). Schematic diagram depicting the MEG process. The two-exciton state,  $|1, q; 1, -q\rangle$ , is generated via the excited states of a single exciton as superposed states of the Coulomb interaction,  $V$ . This results in resonance between the intermediate and final states. Direct generation of the two-exciton state  $|1, q; 1, -q\rangle$  via the exciton-photon interaction  $\mathcal{H}_{\text{op}}$  is forbidden.

then act as intermediate states and resonate with the final states, the two-exciton state with a total momentum  $|1, q; 1, -q\rangle$ , of zero through the Coulomb interaction  $V$ . Finally, a single photon generates two excitons as the final state (i.e., the two-exciton state). Equation (3) shows that energy conservation in MEG does not depend on the excited states of the single exciton since energy is not necessarily conserved between the initial and intermediate states. Therefore, MEG can occur at an excitation energy that satisfies the relation  $\hbar\omega = E_q^1 + E_{-q}^1$ , which is represented by the Dirac delta function. We phenomenologically consider the dephasing processes for the intermediate states by accounting for the dephasing rate  $\gamma$  in the denominator of Eq. (3).

The exciton amplitude  $Z_{k,q}^n$  and energy  $E_q^n$  are obtained by solving the Bethe-Salpeter equation [21,22,28,29]:

$$(\varepsilon_{k+q}^c - \varepsilon_k^v) Z_{k,q}^n + \sum_{k'} K_{k,k'} Z_{k',q}^n = E_q^n Z_{k,q}^n, \quad (4)$$

where  $K_{k,k'}$  is the Coulomb interaction kernel that consists of bare-exchange and screened-direct terms. The quasiparticle energies  $\varepsilon_k^c$  and  $\varepsilon_k^v$  are calculated by applying the random-phase approximation [21,28,29]. For the Coulomb potential between  $\pi$  orbitals, we employed the Ohno potential  $V(\mathbf{r}) = U/\kappa\sqrt{(\frac{4\pi\epsilon_0}{e^2}U|\mathbf{r}|)^2 + 1}$  with  $U = 11.3$  eV, which has been known to realistically describe optical responses in single-walled carbon nanotubes [22,28–30]. The dielectric function  $\kappa = 3.3$  was used to incorporate screening effects by  $\sigma$  electrons and the surrounding environment. The calculations were performed under the tight-binding approximation by accounting for nearest-neighbor hopping of 3.0 eV. We consider a chirality of (17, 0) as a representative of SWNTs.

We start with the conversion rates for one and two-exciton generation. The one-exciton generation rate is given by

$$\Gamma_s(\omega) = \frac{2\pi}{\hbar} \sum_n |\langle n, 0 | \mathcal{H}_{\text{op}} | g \rangle|^2 \delta(\hbar\omega - E_0^n). \quad (5)$$

This is related to linear absorption spectra. Figure 2 shows the conversion rates calculated from Eqs. (3) and (5). The spectral profile for one-exciton generation has the usual structure of the linear absorption spectrum with peaks for the lowest exciton state  $E_{11}$  and higher states and a continuum for excitons above the band gap. In contrast, two-exciton generation increases abruptly at the threshold energy, which corresponds to twice the lowest exciton energy (i.e.,  $2E_{11}$ ). As mentioned above, the threshold energy is solely determined by energy conservation expressed by the Dirac delta function in Eq. (3). Further increasing the excitation energy rapidly reduces the rate. The nature of the spectrum for two-exciton generation can be explained by considering the density of states of the two-exciton state. Because of the quasi-one-dimensional structure of SWNTs, the density of states for excitons possesses van Hove singularities. Thus, the spike at the threshold originates from the van Hove singularity in the density of states for excitons [31]. Furthermore, the rapid reduction in the rates with increasing excitation energy is attributed to a reduction in the density of states. In addition, two-exciton generation strongly depends on the dephasing factor. Figure 2 shows spectra calculated for three representative dephasing factors of  $\gamma = 2.0, 8.0,$  and  $20.0$  meV. The MEG rate decreases rapidly with increasing dephasing rate.

The threshold energy for two-exciton generation has only a single peak since we consider only two-exciton generation. If final states with three or more exciton states are considered, other sharp peaks corresponding to multi-exciton generation will appear.

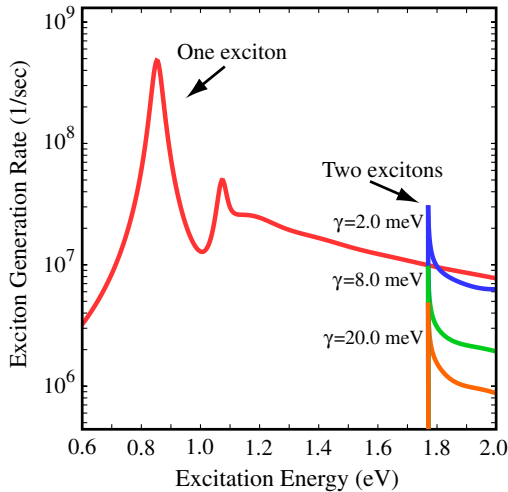


FIG. 2 (color online). Generation rates for one and two excitons by a single photon. The two-exciton generation rates are calculated for dephasing rates of  $\gamma = 2.0, 8.0, 20.0$  meV. The delta functions in Eqs. (3) and (5) were broadened with a width of  $20.0$  meV.

We estimate the conversion efficiency of MEG to investigate whether the process can be used to improve photovoltaic devices. The efficiency is evaluated using the following formula:

$$\eta(\omega) = 1 + \frac{\Gamma_{\text{MEG}}(\omega)}{\Gamma_s(\omega) + \Gamma_{\text{MEG}}(\omega)}, \quad (6)$$

where  $\Gamma_{\text{MEG}}(\omega)$  and  $\Gamma_s(\omega)$  are defined by Eqs. (3) and (5), respectively. Figure 3 shows the calculated conversion efficiencies for dephasing factors of  $\gamma = 2.0, 8.0, 20.0$  meV. The efficiency reaches 175% for  $\gamma = 2.0$  meV, which is close to the maximum efficiency (200%) for two-exciton generation. This remarkably high efficiency is ascribed to both the van Hove singularity in the density of states of the final states and the strong resonance between the intermediate and final states mediated by the Coulomb interaction, which exceeds the dephasing process represented by  $\gamma$ . The MEG efficiency is largest at the threshold energy corresponding to the van Hove singularity, as is the MEG rate (see Fig. 2). Without any dephasing processes, this resonance makes an infinite contribution to the MEG rates. However, as shown in Fig. 3, the MEG efficiency depends strongly on the dephasing factor  $\gamma$  via the denominator of Eq. (3). We note that the linewidth of two-exciton generation peak and the one of single-exciton generation is in generally different with each other. The dephasing rate,  $\gamma$ , of MEG expression Eq. (3) determines the linewidth of single-exciton states. Therefore, the linewidth of two-exciton generation peak around  $2E_{11}$  in Fig. 2 dose not change associated with the dephasing rate  $\gamma$ .

Figure 4 shows the maximum conversion efficiency of MEG as a function of the dephasing rate. It is important to determine how dephasing affects the conversion efficiency. The efficiency decreases monotonically with increasing

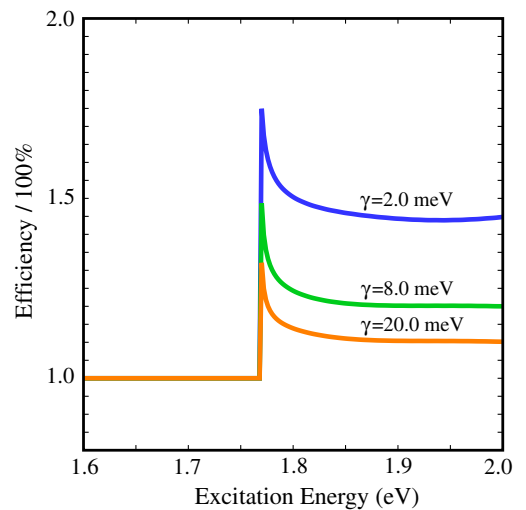


FIG. 3 (color online). Conversion efficiency for direct photo-generation of two excitons plotted for dephasing rates of  $\gamma = 2.0, 8.0,$  and  $20.0$  meV.

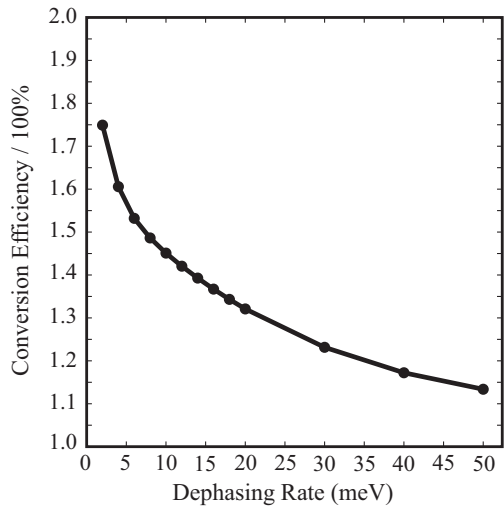


FIG. 4. Dependence of exciton generation rates on the dephasing rate  $\gamma$ .

dephasing rate since dephasing competes with MEG. Assuming a dephasing rate of a few tens of meV (which corresponds to a time of a few femtoseconds) we estimate the conversion efficiency to be about 120%. Thus, MEG has conversion efficiencies of 100% or higher in SWNTs, which raises the possibility of using SWNTs as elemental constituents of photovoltaic devices.

Wang *et al.* recently used transient absorption spectroscopy to observe MEG in SWNTs [25]. They found that the MEG efficiency is about 110% and that the excitation energy is about  $2E_{11}$ . Our calculation based on Eq. (3) predicts that MEG in SWNTs has a threshold energy of  $2E_{11}$ , which agrees exactly with the above experimental result. We can thus conclude that the underlying elementary process of MEG in SWNTs is the direct photogeneration by a single photon.

Finally, we mention that impact ionization [32] has also been proposed as a mechanism for multiple carrier generation [24,33]. Multiple carrier generation results from the delicate balance between the relaxation energy of the higher-energy exciton and the excitation energy of the other exciton. Multiple carrier generation has a threshold energy of  $3E_{11}$ , which is higher than that calculated here for MEG. Obviously, MEG presented in this study differs completely from impact ionization. Their different threshold energies make it possible to distinguish the two processes in SWNTs.

In summary, we have studied MEG in SWNTs. Our calculation has demonstrated that it is possible to generate two excitons by a single photon due to resonant coupling between the optically active one-exciton state and two-exciton states. This resonance is ascribed to the unique characteristics of SWNTs that originate from their quasi-one-dimensional structures, resulting in a strong Coulomb interaction between excitons competing with phonon dephasing and the van Hove singularity in the density of

states of the two-exciton states. Moreover, we have shown that the threshold energy for MEG is exactly  $2E_{11}$ , which is consistent with recent experimental results. The present study clarifies the microscopic process of MEG in SWNTs. Furthermore, it also clarifies the underlying physics of MEG in other materials. MEG raises the possibility of designing high-efficiency photovoltaic devices with low energy consumptions by using SWNTs as constituent units.

This work was supported by CREST of the Japan Science and Technology Agency and a Grant-in-Aid for Scientific Research from the Ministry of Education, Culture, Sports, Science and Technology (MEXT) of Japan.

- [1] W. Shockley and H. J. Queisser, *J. Appl. Phys.* **32**, 510 (1961).
- [2] A. J. Nozik, *Physica (Amsterdam)* **14E**, 115 (2002).
- [3] R. D. Schaller and V. I. Klimov, *Phys. Rev. Lett.* **92**, 186601 (2004).
- [4] R. J. Ellingson, M. C. Beard, J. C. Johnson, P. Yu, O. I. Micic, A. J. Nozik, A. Shabaev, and A. L. Efros, *Nano Lett.* **5**, 865 (2005).
- [5] R. D. Schaller, J. M. Pietryga, and V. I. Klimov, *Nano Lett.* **7**, 3469 (2007).
- [6] M. C. Beard, K. P. Knutsen, P. Yu, J. M. Luther, Q. Song, W. K. Metzger, R. J. Ellingson, and A. J. Nozik, *Nano Lett.* **7**, 2506 (2007).
- [7] J. J. Pijpers, E. Hendry, M. T. W. Milder, R. Fanciulli, J. Savolainen, J. L. Herek, D. Vanmaekelbergh, S. Ruhman, D. Mocatta, and D. Oron, *J. Phys. Chem. C* **112**, 4783 (2008).
- [8] G. Nair, S. M. Geyer, L.-Y. Chang, and M. G. Bawendi, *Phys. Rev. B* **78**, 125325 (2008).
- [9] J. A. McGuire, J. Joo, J. M. Pietryga, R. D. Schaller, and V. I. Klimov, *Acc. Chem. Res.* **41**, 1810 (2008).
- [10] J. J. H. Pijpers, R. Ulbricht, K. J. Tielrooij, A. Osherov, Y. Golan, C. Delerue, G. Allan, and M. Bonn, *Nature Phys.* **5**, 811 (2009).
- [11] J. A. McGuire, M. Sykora, J. Joo, J. M. Pietryga, and V. I. Klimov, *Nano Lett.* **10**, 2049 (2010).
- [12] G. Nair, L.-Y. Chang, S. M. Geyer, and M. G. Bawendi, *Nano Lett.* **11**, 2145 (2011).
- [13] R. D. Schaller, V. M. Agranovich, and V. I. Klimov, *Nature Phys.* **1**, 189 (2005).
- [14] A. Shabaev, A. L. Efros, and A. J. Nozik, *Nano Lett.* **6**, 2856 (2006).
- [15] G. Allan and C. Delerue, *Phys. Rev. B* **73**, 205423 (2006).
- [16] A. Franceschetti, J. M. An, and A. Zunger, *Nano Lett.* **6**, 2191 (2006).
- [17] C. M. Isborn, S. V. Kilina, X. Li, and O. V. Prezhdo, *J. Phys. Chem. C* **112**, 18291 (2008).
- [18] E. Rabani and R. Baer, *Chem. Phys. Lett.* **496**, 227 (2010).
- [19] W. M. Witzel, A. Shabaev, C. S. Hellberg, V. L. Jacobs, and A. L. Efros, *Phys. Rev. Lett.* **105**, 137401 (2010).

- [20] K. A. Velizhanin and A. Piryatinski, *Phys. Rev. Lett.* **106**, 207401 (2011).
- [21] T. Ando, *J. Phys. Soc. Jpn.* **66**, 1066 (1997).
- [22] V. Perebeinos, J. Tersoff, and P. Avouris, *Phys. Rev. Lett.* **92**, 257402 (2004).
- [23] C.D. Spataru, S. Ismail-Beigi, L. X. Benedict, and S. G. Louie, *Phys. Rev. Lett.* **92**, 077402 (2004).
- [24] A. Ueda, K. Matsuda, T. Tayagaki, and Y. Kanemitsu, *Appl. Phys. Lett.* **92**, 233105 (2008).
- [25] S. Wang, M. Khafizov, X. Tu, M. Zheng, and T. D. Krauss, *Nano Lett.* **10**, 2381 (2010).
- [26] N.M. Gabor, Z. Zhong, K. Bosnick, J. Park, and P.L. McEuen, *Science* **325**, 1367 (2009).
- [27] F. Wang, Y. Wu, M. S. Hybertsen, and T.F. Heinz, *Phys. Rev. B* **73**, 245424 (2006).
- [28] T. Ando, *J. Phys. Soc. Jpn.* **75**, 024707 (2006).
- [29] J. Jiang, R. Saito, Ge. G. Samsonidze, A. Jorio, S.G. Chou, G. Dresselhaus, and M. S. Dresselhaus, *Phys. Rev. B* **75**, 035407 (2007).
- [30] R.B. Capaz, C.D. Spataru, S. Ismail-Beigi, and S.G. Louie, *Phys. Rev. B* **74**, 121401 (2006).
- [31] C.L. Kane and E.J. Mele, *Phys. Rev. Lett.* **90**, 207401 (2003).
- [32] V. Perebeinos and P. Avouris, *Phys. Rev. B* **74**, 121410(R) (2006).
- [33] R. Baer and E. Rabani, *Nano Lett.* **10**, 3277 (2010).